

Growth and optical properties of phosphorus-doped ZnO nanowires

D.S. Kim^{a,*}, J. Fallert^b, A. Lotnyk^a, R. Scholz^a, E. Pippel^a, S. Senz^a, H. Kalt^b, U. Gösele^a,
M. Zacharias^{a,c}

^a Max-Planck-Institute of Microstructure Physics, Weinberg 2, 06120 Halle, Germany

^b Universität Karlsruhe, Institut für Angewandte Physik, Wolfgang-Gaede-Straße 1, 76131 Karlsruhe, Germany

^c IMTEK, Faculty of Applied Science, Albert-Ludwigs-University Freiburg, Georges-Köhler-Allee, 79110 Freiburg, Germany

Received 14 February 2007; received in revised form 28 May 2007; accepted 28 June 2007 by J.W.P. Hsu

Available online 17 July 2007

Abstract

Single-crystal phosphorus-doped ZnO nanowires were synthesized by using a single-source precursor-based vapor transport method. The photoluminescence spectra of phosphorus-doped ZnO nanowires and undoped nanowires are compared. While both show several shallow bound exciton complexes, the phosphorus-doped nanowires reveal an additional distinct emission feature at 3.316 eV. Additionally, the time-resolved PL measurements were conducted to characterize the recombination dynamics.

© 2007 Elsevier Ltd. All rights reserved.

PACS: 78.66.-w; 78.66.Hf; 78.47.+p

Keywords: A. Semiconductors; A. Nanostructures; C. Scanning and transmission electron microscopy; D. Optical properties

1. Introduction

ZnO nanowires with a direct band gap of 3.44 eV and a large exciton binding energy of 60 meV, have attracted increasing interest due to its potential applications in electronics and optoelectronics. Recently, a light-emitting diode (LED) based on a ZnO homojunction film was demonstrated [1,2]. It was the result of the reliable *p*-type doping of ZnO with a high concentration of nitrogen ($\sim 10^{20} \text{ cm}^{-3}$) and a low-defect density. Devices based on ZnO nanowires could provide an alternative nanoscale UV light source. The synthesis of reliable *p*-type ZnO nanowires is thus desired. Despite its importance, only few results on the doping of ZnO nanowires have been reported so far [3–5].

In this paper, we demonstrate a versatile growth technique to synthesize phosphorus-doped ZnO (ZnO:P) nanowires in a reproducible way. With this approach, we are able to prepare phosphorus-doped single-crystal ZnO nanowires. We will discuss the detailed optical properties of phosphorus-doped ZnO nanowires based on low-temperature photoluminescence (PL) and time-resolved PL (TRPL).

2. Experimental details

In the typical growth process, ZnO:P nanowires are synthesized via a vapor transport process based on a single-source precursor, Zn_3P_2 . In the approach presented here, Zn_3P_2 is used as source for both Zn and P. In order to meet the conditions of the sublimation of Zn_3P_2 and the formation of the liquid droplet of Au catalyst, the temperature at the source boat and the substrate were controlled at $\sim 500^\circ\text{C}$ and 800°C , respectively. The details are as follows: an alumina boat containing the Zn_3P_2 powder and a Si substrate covered with a 5 nm Au film were placed in a small quartz tube, separated typically by 7–10 cm. This small quartz tube was then placed inside a horizontal tube furnace, where the source boat was positioned upstream from the substrate and located in front of the heating zone. A constant pressure was maintained during the growth process with an Ar gas of flow rate 30 sccm. The temperature of the furnace was set to 800°C and typically kept at the maximum temperature for 40 min.

For comparison, undoped ZnO nanowires were also produced. Here, ZnO nanocrystals, which were prepared by a chemical solution deposition (CSD), were used for nanowire nucleation instead of a metal catalyst. The 0.75 M precursor

* Corresponding author. Tel.: +49 345 5582 641; fax: +49 345 5511 223.
E-mail address: dskim@mpi-halle.de (D.S. Kim).

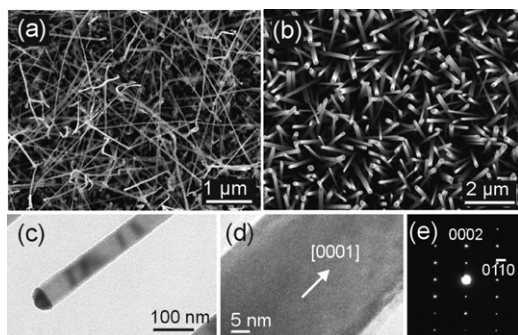


Fig. 1. SEM images of ZnO:P nanowires based on Au-assisted growth (a), and ZnO nanowires based on ZnO nanocrystals-assisted growth (b). (c) TEM image of a ZnO:P nanowire. (d) High-resolution TEM image of the ZnO:P nanowire. (e) The corresponding SAED pattern.

solution, which was prepared by stirring the components zinc acetate dihydrate and monoethanolamine in a molar ratio of 1:1 in 2-methoxyethanol for 3 h at 80 °C under Ar gas was deposited onto the Si substrate by spin coating. The as-deposited films were then preheated on a hotplate at 300 °C for 10 min. Finally the sample was annealed at 500 °C for 1 h. For nanowire growth, ZnO powder (Alfa Aesar, 99.999%) and graphite powder (Alfa Aesar, 99.9995%) were ground together (1:1 wt%) and loaded into an alumina boat. The substrate covered with the ZnO nanocrystal layer and the alumina boat were placed into a small quartz tube, separated typically by 10–11 cm. This small quartz tube was then placed inside a furnace quartz tube with the source boat positioned at the center of the heating zone and the substrate placed downstream of an Ar flow. The temperature of the furnace was set to 925 °C and typically kept at the maximum temperature for 30 min under a constant flow of Ar with 30 sccm. After the growth, the furnace was cooled to room temperature.

3. Results and discussion

The morphologies of the as-grown ZnO:P nanowires and ZnO nanowires were investigated using scanning electron microscopy (SEM). As shown in Fig. 1(a), entangled and uniform ZnO:P nanowires were grown on the Si substrate. The diameters of the nanowires range from 40–80 nm and their lengths reach a few micrometers. Fig. 1(b) shows quasi-aligned ZnO nanowires with well-defined facets on the Si substrate. The nanowires have a typical diameter of 30–100 nm and a length of a few micrometers. All wires are terminated by a flat plane. Transmission electron microscopy (TEM) analysis revealed that most of the ZnO:P nanowires are terminated by Au nanoparticles, indicating that ZnO:P nanowires were grown via a Au-assisted vapor–liquid–solid (VLS) process. Fig. 1(c) shows a representative TEM image of a ZnO:P nanowire. Fig. 1(d) shows a high-resolution TEM image of a ZnO:P nanowire with clearly resolved lattice fringes, confirming their crystallinity. Fig. 1(e) shows a selected-area electron diffraction (SAED) pattern obtained from a representative ZnO:P nanowire. It demonstrates that the nanowire is single-crystalline with a wurtzite structure and a growth direction along [0001].

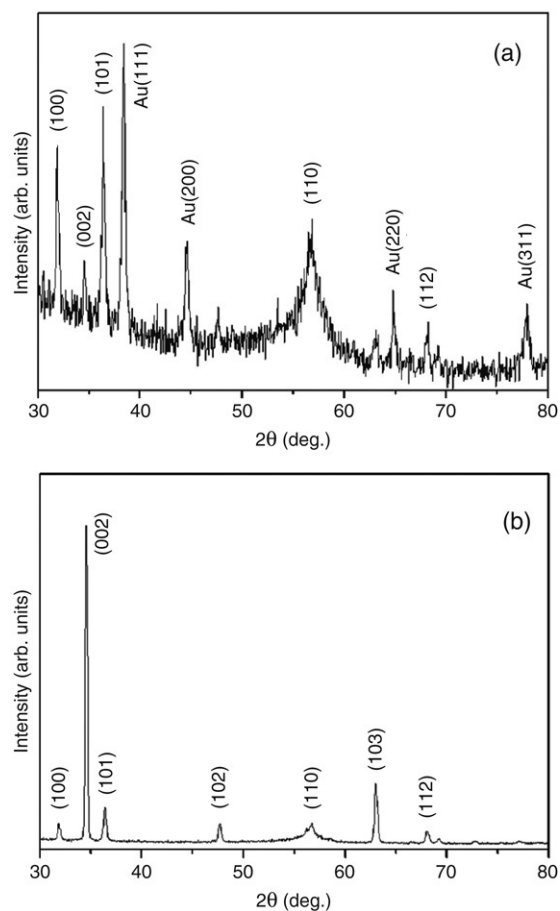


Fig. 2. XRD pattern of as-grown ZnO:P nanowires (a), and ZnO nanowires (b). The peaks of the Au used as catalyst can be seen in the sample of the doped wires.

In addition, Fig. 2(a) shows the X-ray diffraction (XRD) pattern of ZnO:P nanowires which confirms that no secondary phase exists in ZnO:P nanowires. In case of undoped ZnO nanowires, a typical XRD pattern of the hexagonal ZnO was observed as shown in Fig. 2(b).

The overall composition and the spatial distribution of phosphorus atoms in individual nanowires were investigated by energy-dispersive X-ray (EDX) spectroscopy. 4.3 at.% of phosphorus was detected at the Au-based metallic particles, located at the tip of ZnO:P nanowires. However due to the sensitivity limit of EDX (not better than approximately 1 at.%), we are not able to estimate the phosphorus content in the nanowires reliably. The EDX analysis of *p*-type GaN nanowires was also not sensitive enough to show the presence of Mg dopants [6]. Because of the difficulties in elemental analysis and electrical device fabrications for the quantitative analysis of the dopant concentration, we used low-temperature PL to prove and characterize the presence of phosphorus dopants in ZnO:P nanowires. PL spectroscopy is a very sensitive and nondestructive tool for investigating metal impurities in semiconductor nanowires [7].

PL of the samples was measured using the 325 nm line of a HeCd laser as excitation source with an intensity of ~ 4 W/cm². The low-temperature PL spectra of ZnO:P and ZnO nanowires

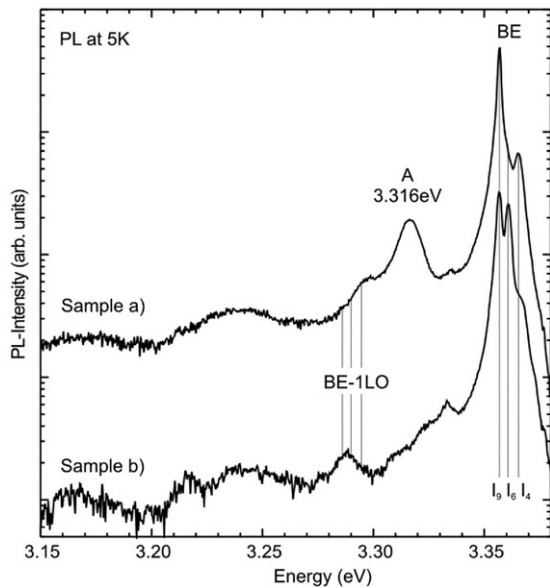


Fig. 3. Low-temperature PL spectra of as-grown ZnO:P nanowires (sample a), and ZnO nanowires (sample b), respectively.

are compared in Fig. 3. In the used liquid He-bath cryostat, a temperature of 5 K was measured in a thermal equilibrium of the copper sample holder with the attached sensor and the sample fixed on it by a heat-conducting glue. The spectrum of undoped ZnO nanowires shows typical transition features. In the present case, the strong emissions observed between 3.357 and 3.363 eV are bound exciton transitions (BE). These lines are typically labeled as I_4 (3.363 eV), I_6 (3.361 eV) and I_9 (3.357 eV) [8].

In the case of ZnO:P nanowires, the PL spectrum is again dominated by emission from shallow BE. Additionally, another emission band at 3.316 eV is observed, which is not found in the undoped ZnO nanowires. This band is in the following denoted by the letter A. Such an emission band around 3.31 eV has on one hand been reported in *p*-type nitrogen [9,10] or phosphorus [11,12] doped ZnO film. On the other hand such an emission band was also found in nominally undoped samples [11,15] and is strongly present in ZnO nanocrystals [15]. So far the physical origin of this emission is still unclear. But from our results it seems likely that this additional state is caused by the presence of phosphorus atoms in the ZnO nanowires.

Time-resolved PL (TRPL) spectroscopy was used to examine the time-dependent carrier dynamics in ZnO:P and ZnO nanowires. The signal was recorded by the use of a streak camera with a temporal resolution of 5 ps. The excitation in those measurements is accomplished by 150 fs pulses of a frequency doubled Ti:Sapphire-laser at 360 nm. In the TRPL measurement a He-flow cryostat was used and in thermal equilibrium a temperature of 13 K was measured. The decay curves of the radiative emission at the BE energy of 3.357 eV (I_9) and the A peak at 3.316 eV were monitored in Fig. 4. Both peaks show a biexponential decay, with a rapid decay component in the beginning. This is caused by the high-carrier densities shortly after the excitation pulse with several $\mu\text{J}/\text{cm}^2$.

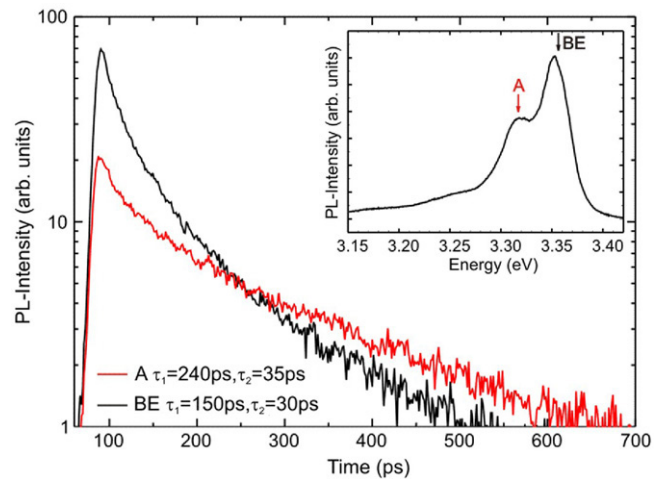


Fig. 4. Decay curves from time-resolved PL spectra of the BE and A emission peaks in ZnO:P nanowires. The inset shows the time-integrated PL spectrum.

Therefore also the time-integrated PL spectrum, as shown in the upper right corner of Fig. 4, is broadened compared to the continuous wave PL measurement. The two emission bands which can be seen in the time-integrated spectrum are present at all times. While at earlier times the BE peak is dominant, the A peak contributes mainly to the emission with a monoexponential tail with a lifetime of about 240 ps at later times.

For unequivocally demonstrating that the incorporated phosphorus atoms actually lead to *p*-type doping as expected, further electrical measurements are required, and this is in progress. In general, implantation, diffusion and *in situ* doping during vapor phase or MBE growth have been adopted as methods of *p*-type doping in ZnO films. Our route to incorporate dopants in ZnO nanowires is, however, quite different from such ways of doping ZnO films. Phosphorus is incorporated into the nanowire lattice via the liquid alloy (Au–Zn) e.g., liquid-phase-assisted *in situ* doping not a vapor phase *in situ* doping. In this doping mode, the liquid–solid interface provides a low-energy site (e.g., a sink for the dopant), and facilitates the transport of dopants from the vapor to the crystal. Although all *p*-type dopants have a fairly low solubility in the ZnO lattice [13], we were able to grow phosphorus-doped ZnO nanowires. In addition, grown nanowires show no tapering. Since a few atomic layers of dopants deposited on the surface of a nanowire can dominate its overall electronic properties, dopant induced tapering is undesirable [14].

4. Conclusions

In summary, phosphorus-doped ZnO nanowires were synthesized by using a vapor transport process. Based on a single-source precursor, Zn_2P_3 , single-crystal phosphorus-doped ZnO nanowires were produced in a reproducible way. Low-temperature PL spectra show that the presence of phosphorus strongly enhances a peak at 3.316 eV. We suggest that Au catalyst plays an important role for doping in ZnO nanowires.

Acknowledgements

This work was supported by the International Max Planck Research School for Science and Technology of Nanostructures (Nano-IMPRS) in Halle, the Deutsche Forschungsgemeinschaft (DFG) and the Landeskompetenznetz Baden-Wuerttemberg within the Competence Network 'Functional Nanostructures', Project A1.

References

- [1] A. Tsukazaki, T. Onuma, M. Ohtani, T. Makino, M. Sumiya, K. Ohtani, S.F. Chichibu, S. Fuke, Y. Segawa, H. Ohno, H. Koinuma, M. Kawasaki, *Nat. Mater.* 4 (2005) 42.
- [2] A. Tsukazaki, M. Kubota, A. Ohtomo, T. Onuma, K. Ohtani, H. Ohno, S.F. Chichibu, M. Kawasaki, *Japan J. Appl. Phys., Part 2* 44 (2005) L643.
- [3] W. Lee, M.-C. Jeong, J.-M. Myoung, *Acta Mater.* 52 (2004) 3949.
- [4] J.H. Park, I.S. Hwang, Y.J. Choi, J.G. Park, *J. Cryst. Growth* 276 (2005) 171.
- [5] C.-L. Hsu, S.-J. Chang, Y.-R. Lin, S.-Y. Tsai, I.-C. Chen, *Chem. Commun.* (2005) 3571.
- [6] Z. Zhong, F. Qian, D. Wang, C.M. Lieber, *Nano Lett.* 3 (2003) 343.
- [7] J. Yoo, Y.-J. Hong, S.J. An, G.-C. Yi, B. Chon, T. Joo, J.-W. Kim, J.-S. Lee, *Appl. Phys. Lett.* 89 (2006) 043124.
- [8] B.K. Meyer, H. Alves, D.M. Hofmann, W. Kriegseis, D. Forster, F. Bertram, J. Christen, A. Hoffmann, M. Straßburg, M. Dworzak, U. Habocek, A.V. Rodina, *Phys. Status Solidi B* 241 (2004) 231.
- [9] D.C. Look, D.C. Reynolds, C.W. Litton, R.L. Jones, D.B. Eason, G. Cantwell, *Appl. Phys. Lett.* 81 (2002) 1830.
- [10] X.D. Yang, Z.Y. Xu, Z. Sun, B.Q. Sun, L. Ding, F.Z. Wang, Z.Z. Ye, *J. Appl. Phys.* 99 (2006) 046101.
- [11] F.X. Xiu, Z. Yang, L.J. Mandalapu, J.L. Liu, W.P. Beyermann, *Appl. Phys. Lett.* 88 (2006) 052106.
- [12] F.X. Xiu, Z. Yang, L.J. Mandalapu, J.L. Liu, *Appl. Phys. Lett.* 88 (2006) 152116.
- [13] C.G. Van de Walle, D.B. Laks, G.F. Neumark, S.T. Pantelides, *Phys. Rev. B* 47 (1993) 9425.
- [14] A.B. Greytak, L.J. Lauhon, M.S. Gudiksen, C.M. Lieber, *Appl. Phys. Lett.* 84 (2004) 4176.
- [15] J. Fallert, R. Hauschild, F. Stelzl, A. Urban, M. Wissinger, H. Zhou, C. Klingshirn, H. Kalt, *J. Appl. Phys.* 101 (2007) 73506.